APMP Key Comparison Report of Reference air kerma rate for HDR ^{192}Ir brachytherapy sources (BIPM KCDB: APMP.RI(I)-K8)

J. Ishii[a], T. Kurosawa[a], M. Kato[a], P. Toroi[b], W.-H. Chu[c], C.-Y. Yi[d], Y. H. Kim[d], Y. M. Seong[d] S. A. Ngcezu[e], E. Mainegra-Hing[f], B. Downton[f], M. T. Dolah[g], C. T. Budiantari[h]

[a]*National Metrology Institute of Japan, Tsukuba, Japan*

[b]*International Atomic Energy Agency, Vienna, Austria*

[c]*Institute of Nuclear Energy Research, Longtan, Taiwan*

[d]*Korea Research Institute of Standards and Science, Yusong, Korea*

[e]*National Metrology Institute of South Africa, Pretoria, South Africa*

[f]*National Research Council of Canada, Ottawa,Canada*

[g]*Malaysian Nuclear Agency (Nuclear Malaysia), Kajang, Malaysia*

[h]*National Atomic Energy Agency (BATAN), Jakarta, Indonesia*

Abstract

The APMP/TCRI Dosimetry Working Group performed the APMP.RI(I)-K8 key comparison of the reference air kerma rate for high-dose-rate (HDR) ^{192}Ir brachytherapy sources between 2016 and 2018. Eight laboratories, including seven national metrology institutes (NMIs), took part in the comparison. Two commercial well-type chambers were used as transfer instruments and circulated among the participants. The results showed that the maximum difference between the participants and the BIPM, evaluated using the comparison data of the linking laboratories NMIJ and NRC, was less than 4%. The degrees of equivalence for the participants were calculated, so that results for the six non-linking laboratories may be included in the Key Comparison Database (KCDB).

1. Introduction

Brachytherapy using high-dose-rate (HDR) ^{192}Ir is a type of radiation treatment that works by placing a source very close to (usually inside) a patient's body to destroy cancer cells. The strength of the source is characterized by the reference air kerma rate

(RAKR or $\dot{K}_R$) and measured by instruments which are traceable to national standards in each NMI or the BIPM.

This comparison was performed to establish the degrees of equivalence between these standards, and thereby support the validity of the standards and calibration services at each laboratory. For this purpose, it was proposed to use two well-type ionization chambers (of the type commonly calibrated for clinical use by standards laboratories) as the transfer instruments. The calibration coefficients of the transfer instruments were measured by each participant. Eight laboratories took part in the comparison: IAEA (International Organization), INER (Taiwan), KRISS (Korea), NMIJ (Japan), NMISA (South Africa), NRC (Canada), Nuclear Malaysia (Malaysia) and PKTMR-BATAN (Indonesia). The contact persons of the laboratories are listed in Table 1. Two of the participating laboratories, the NMIJ and the NRC, also took part in the international key comparison BIPM.RI(I)-K8 organized by the BIPM [1]; the corresponding results have been used to link the APMP/TCRI regional comparison to the international comparison. Therefore, the reference value for this key comparison is the BIPM reference value.

The comparison was arranged by the NMIJ as the pilot laboratory. The circulation of the transfer chambers among the participants followed a ring-shaped path. However, the chambers were returned to NMIJ, as planned, after the first participant NRC as a check of the procedures, before they completed the loop. The circular path reduces the number of times the instruments have to be processed by customs. In order to reduce the risk of chamber drift affecting the results, participants were requested to complete their measurements in one week. The schedule of the comparison is shown in Table 2. NMIJ measured the calibration coefficients at the beginning, and near the completion of the comparison, as a check on the chamber stability. The KRISS travelled to NMIJ with their primary standard to perform their measurements immediately after the final stability check. The comparison started in September 2016 and measurements were completed in September 2018.

2. Procedure

2.1 Transfer chambers

Two well-type ionization chambers and two holders (Standard Imaging HDR

1000 Plus, ref. 90008, with Standard Imaging HDR Iridium Source Holder, ref. 70010) were used as transfer standards for the comparison: serial numbers A153466 and A983216. The characteristics of this chamber type are listed in Table 3. The electrical connection of the chambers is via a tri-axial BNT plug. Participants used their own charge/current measuring system (electrometer) to provide a bias voltage and read the signal. The protocol specified the warm-up time for an electrometer to be more than 12 hours, and the chamber to be connected to the electrometer and bias applied more than 1 hour before measurements. The protocol requested a pre-irradiation of the chamber for around 5 minutes, which was performed before starting measurements. The chambers are air-communicating and the instructions included checking that the vent hole in the chamber housing was not blocked.

2.2 Reference conditions and measurement procedure

The measured charges/currents were normalized to the reference environmental conditions of 20 °C and 101.325 kPa. The reference relative humidity was 50 %.

The protocol specified that the calibration coefficient must be measured with the source inserted to the point of maximum chamber response (the "sweet spot"). Each laboratory determined the sweet spot by stepping the brachytherapy source through the well-chamber in steps of a few millimeters and plotting the measured ionization current against the dwell positions to find the position corresponding to the maximum current.

The protocol also recommended that the well-chamber be placed on a low scatter support at a distance of 1 meter or more from any wall and from the floor of the calibration room [2].

2.3 HDR ^{192}Ir brachytherapy source

Each laboratory calibrated the transfer standards using its own ^{192}Ir brachytherapy source. The characteristics of these sources are given in Table 4. Before the comparison started, the NMIJ performed a preliminary test to check the difference between microSelectron mHDR-V2 and Varian Varisource VS2000 source types. Published differences are as large as 1.7% [3] and 1.6% [4], and NMIJ measured a difference of 0.8% (see section 3.2).

2.4 Calibration coefficients measured by the participants

The calibration coefficients of the transfer chambers for reference air kerma rate

are expressed in units of Gy m^2 h^{-1} A^{-1} and are defined with the source positioned at the "sweet spot" (point of maximum response). Each participant calibrated the transfer chambers using their own ^{192}Ir source: traceability to a national standard and methods to determine the reference air kerma are given in Table 5. After the sweet spot position had been determined by the participant, the ionization current was measured with the participant's electrometer, corrected to the reference temperature and pressure, corrected for source decay to the participant's reference date, and corrected for ion recombination. Note that participants could measure current directly or integrate charge over a fixed period, according to their local procedures.

The calibration coefficient $N_{K,\mathrm{NMI}}$ for the well-type chamber is expressed as

$$N_{K,\mathrm{NMI}} = \frac{\dot{K}_{\mathrm{R,NMI}}}{(M_{\mathrm{raw}} - M_{\mathrm{leak}}) \cdot k_{\mathrm{ele}} \cdot k_{\mathrm{ion}} \cdot k_{\mathrm{dec}} \cdot k_{PT}} \qquad (1)$$

where:

$\dot{K}_{\mathrm{R,NMI}}$: the RAKR determined at the NMI with the reference standard/method

M_{raw} : the raw current measured at the NMI without any correction

M_{leak} : the measured leakage current

k_{ele} : the calibration coefficient of the participant's electrometer

k_{ion} : the correction factor for ion recombination in the well-chamber, which can be estimated by using the two-voltage technique

k_{dec} : the correction factor for radioactive decay of the source, between the comparison measurements and the date when $\dot{K}_{\mathrm{R,NMI}}$ was determined, using the laboratory's value of the half-life.

k_{PT} : the correction factor for atmospheric conditions.

No correction was required for any polarity effect. k_{ion} for continuous radiation was calculated using the following equation [5].

$$k_{\mathrm{ion}} = \frac{(V_1/V_2)^2 - 1}{(V_1/V_2)^2 - M_1/M_2} \qquad (2)$$

where:

V_1: Applied voltage for normal operation (Collecting Electrode Positive)

V_2 : Reduced applied voltage for ion recombination measurement, where $V_2 = V_1/2$ (Collecting Electrode Positive)

M_1: Measured current at V_1

M_2: Measured current at V_2.

2.5 Evaluation of measurement uncertainty

All the participating laboratories have estimated the uncertainty of their calibration coefficients according to the "Guide to The Expression of Uncertainty in Measurement" [6], noting that Type A uncertainties are obtained by the statistical analysis of a series of observations, and the Type B uncertainty are obtained by means other than the statistical analysis of a series of observations. In order to analyze the uncertainties and take correlations into account for degrees of equivalence entered in the BIPM key comparison database, the participating laboratories submitted their detailed uncertainty budgets to the pilot laboratory (see Appendix I).

2.6. The linking of regional comparisons to international comparisons

Two of the participating laboratories, the NMIJ and the NRC, took part in the international key comparison organized by the BIPM, BIPM.RI(I)-K8, in 2015. To link the APMP/TCRI comparison (a regional comparison) with the BIPM comparison result, NMIJ and NRC were to play the role of "linking laboratory". The measured calibration coefficients for each laboratory were converted to ratios $\overline{R_{\mathrm{NMI,BIPM}}}$ relative to the reference value reported in the international key comparison with BIPM.

The comparison results of each participating NMI were evaluated for each linking laboratory i (i = NMIJ, NRC) as

$$R_{\mathrm{NMI,LINK}_i} = \frac{1}{2}\left(\frac{N_{\mathrm{NMI},j1}}{N_{\mathrm{LINK}_i,j1}} + \frac{N_{\mathrm{NMI},j2}}{N_{\mathrm{LINK}_i,j2}}\right) \tag{3}$$

where $N_{\mathrm{NMI},j1}$, $N_{\mathrm{NMI},j2}$, $N_{\mathrm{LINK}_i,j1}$ and $N_{\mathrm{LINK}_i,j2}$ are the calibration coefficients obtained in the present comparison. In this equation, $j1$ and $j2$ refer to the transfer chambers, respectively. The ratio of the calibration coefficient between each participating NMI and the BIPM reference value for each linking laboratory i as

$$\left(R_{\mathrm{NMI,BIPM}}\right)_i = R_{\mathrm{NMI,LINK}_i} \cdot R_{\mathrm{LINK}_i,\mathrm{BIPM}} \tag{4}$$

In this equation, $R_{\mathrm{LINK}_i,\mathrm{BIPM}}$ is the ratio of the calibration coefficient to the reference value reported in the BIPM.RI(I)-K8 comparison result, as listed in Table 6. As there are two linking laboratories, this results in two values $\left(R_{\mathrm{NMI,\,BIPM}}\right)_i$ and the unweighted

mean value is calculated using the following equation.

$$\overline{R_{\mathrm{NMI,BIPM}}} = \frac{1}{2}\sum_i \left(R_{\mathrm{NMI,\,BIPM}}\right)_i \qquad (5)$$

The uncertainty $u_{R,\,\mathrm{NMI}}$ of this mean value takes the correlation between the NMI and BIPM standards into account using the following equation [7].

$$u^2_{R,\mathrm{NMI}} = \left(u^2_{\mathrm{NMI}} + u^2_{\mathrm{BIPM}} - \sum_n f_n^2\left(u^2_{\mathrm{NMI},n} + u^2_{\mathrm{BIPM},n}\right)\right) + u^2_{\mathrm{stab}} + u^2_{\mathrm{LINK}} \qquad (6)$$

In this equation, the summation contains those components correlated between each NMI and the BIPM, with correlation factor f_n. The u_{stab} was evaluated from the stability measurements at the NMIJ. The statistical uncertainty of the linking procedure, u_{LINK_i}, is evaluated for each linking laboratory i, and the use of two linking laboratories reduces the combined value (used in the above equation) according to

$$u_{\mathrm{LINK}} = \frac{1}{2\sqrt{2}}\sum_i u_{\mathrm{LINK}_i} \qquad (7)$$

However, the two values $\left(R_{\mathrm{NMI,\,BIPM}}\right)_i$ do not agree at this level (0.37%). An alternative estimate of u_{LINK} can be obtained from the difference between the linking laboratories using equation 7 of reference [8], which yields a value of 0.60%:

$$u^2_{\mathrm{LINK}} = \frac{1}{1.2}\sum_i \left(R_{\mathrm{NMI,\,BIPM}_i} - \overline{R_{\mathrm{NMI,BIPM}}}\right)^2 . \qquad (8)$$

For each NMI having a comparison result $\overline{R_{\mathrm{NMI,BIPM}}}$ with combined standard uncertainty, $u_{R,\mathrm{NMI}}$, the degree of equivalence with respect to the BIPM reference value is $D_i = \overline{R_{\mathrm{NMI,BIPM}}} - 1$ and its expanded uncertainty $U_i = 2u_{R,\mathrm{NMI}}$.

3. Results

3.1 Stability of transfer standards

The verification of the two transfer chamber stabilities was performed at the pilot laboratory, the NMIJ. The standard deviation to the mean values of the calibration coefficients (combining both chambers) before and after the comparison measurements, u_{stab}, was found to be less than 0.01%.

3.2 Source model effects

The participants used their own HDR afterloader and source (Table 4). These sources are nearly identical (capsule dimensions approximately 0.9 mm in diameter and 4.5 mm in length). We therefore expect that any differences due to the source model will be small. However, we acknowledge that differences may exist, and note that we have not applied any corrections to the comparison results for the different afterloaders or sources.

At NMIJ there is a second HDR unit with a different source: the Varian Varisource VS2000. This source has a capsule 0.59 mm in diameter and 7.05 mm in length. The difference in the well-chamber calibration coefficients obtained at NMIJ for this source and the microSelectron mHDR-V2 was 0.8%, with a higher calibration coefficient obtained with the Varian Varisource. This result illustrates the magnitude of the differences that are possible, and we expect differences between sources of similar geometry to be much less than this. The NMIJ result using the microSelectron mHDR-V2 source was used in the comparison.

The results of IAEA were obtained with a stainless steel needle (Model LLA210-S by Eckert & Ziegler BEBIG, outer diameter 1.5 mm, wall thickness 0.2 mm). This was allowed under the comparison protocol which differs from the BIPM key comparison protocol. The needle was used to fit the IAEA source into the provided source holder. IAEA considers the calibration coefficient would be lower by a factor of 0.992, based on their experimental results, if the needle was not used. The IAEA calibration coefficients in this report therefore include the correction of 0.992.

3.3 Calibration coefficients

The calibration coefficients for the transfer chambers in each participating laboratory are given in Table 6. The detailed uncertainty budgets for all the participants are given in the Appendix. This comparison started prior to ICRU report 90 being published, hence data in this report do not take its recommendations into account. For each chamber, the mean and the standard deviation of the distribution of the calibration coefficients are evaluated. Figure 1, produced using the data of Table 7, shows no unexpected behavior, with all calibration coefficients falling within two standard deviations of the mean and no significant outliers identified.

Unweighted mean values have been used to combine the data for the two transfer chambers and for the two linking laboratories. Tables 8 and 9 show the comparison

results for each laboratory to each of the linking laboratories NMIJ and NRC. The links to BIPM are separately evaluated by the NMIJ and the NRC; the relative difference of the two ratios $\left(R_{\mathrm{NMI,\,BIPM}}\right)_i$ is 0.93%. This difference is consistent with the combined standard uncertainties of each ratio indicating reasonable but not ideal agreement between the two linking mechanisms.

Although the results of this comparison and the previous comparison between NMIJ and BIPM were obtained by measurement of well-type chambers, the comparison result between NRC and BIPM was obtained from thimble chambers. Both of these linking comparisons link to the same reference value (the BIPM thimble chamber). However, they do so through quite different mechanisms. The well-chamber route uses the average of the well-chamber calibration coefficient derived from (as of 2021) four BIPM key comparisons, those with VSL, NPL, PTB and NRC. The uncertainty estimate from the linking comparisons (NMIJ and NRC) is 0.37% from Equation (7). We have treated the two linking uncertainties as uncorrelated.

The alternative estimate of the uncertainty in the linking mechanism may be obtained from the difference between the two linking results, using equation (8) to obtain u_{LINK} = 0.60%, which we have used in this analysis. The difference between the links suggests the presence of an un-accounted for uncertainty. This could possibly be related to the non-uniformity correction for the thimble chamber when used close to the source, which is accounted for in different ways by the BIPM comparison participants, or possibly a contribution from source replacements (although the same model was always used, the sources would have been replaced between the BIPM and APMP comparisons).

The mean ratios calculated from Tables 8 and 9 are the final comparison results $\overline{R_{\mathrm{NMI,BIPM}}}$ for each laboratory relative to the BIPM, as given in Table 10 and Figure 2. The largest deviation from the BIPM value in Figure 2 is approximately 4%, which is the result of PTKMR-BATAN, but the distribution of deviations, except PTKMR-BATAN, falls within 2%. The combined standard uncertainty $u_{R,\mathrm{NMI}}$ of $\overline{R_{\mathrm{NMI,BIPM}}}$ for each laboratory is also given in Table 10. The results for the degrees of equivalence, D_i and U_i are shown in Table 11 and Figure 3, expressed in mGy/Gy. It should be noted that for consistency within the KCDB, a simplified level of nomenclature is used in these tables with $R_{i,\mathrm{BIMP}}$ equivalent to $x_i/x_{R,i}$.

We note that the relatively large (0.6%) contribution from the linking mechanism

results in a greater uncertainty component of the degrees of equivalence than might be obtained in a direct comparison. Nevertheless, the demonstration of equivalence is important for the laboratories, and can be used to support CMC claims which are consistent with the equivalence demonstrated here.

4. Conclusion

A comparison of the reference air kerma rate for HDR ^{192}Ir brachytherapy sources has been carried out among eight laboratories. Two well-chamber transfer standards were circulated among the eight laboratories and each laboratory was asked to provide calibration coefficients and associated uncertainties. The stabilities of the chambers were measured at NMIJ before and after the comparison. For both well-chambers the stability was shown to be within 0.01%. The comparison results showed the calibration capabilities of all participating laboratories to be in general agreement within the stated uncertainties. The APMP comparison results, except PTKMR-BATAN, agreed with the BIPM reference value within the expanded uncertainties (k = 2), and the PTKMR-BATAN was only just outside the expanded uncertainty. This comparison established the degrees of equivalence of the calibration and measurement capability of the participating laboratories.

References

[1] BIPM.RI(I)-K8 Technical Protocol, Version 6.0, July 2014, https://www.bipm.org/kcdb/comparison?id=285

[2] Chang, L., Ho, S. Y., Chui, C. S., Lee, J. H., Du, Y. C. and Chen, T., A statistical approach to infer the minimum setup distance of a well chamber to the wall or the floor for ^{192}Ir HDR calibration Med. Phys.,2008, 35, 2214-2216.

[3] Shipley, D. R., Sander, T., Nutbrown, R. F., Source geometry factors for HDR ^{192}Ir brachytherapy secondary standard well-type ionization chamber calibrations. Phys. Med. Biol.,2015, 60 (6), 2573.

[4] Rasmussen. B. E., Davis. S. D., Schmidt. C. R., Micka, J. A. and DeWerd, L. A., Comparison of air-kerma strength determinations for HDR ^{192}Ir sources, Med. Phys.,2011, 38, 6721–6729.

[5] Andreo, P., Burns, D. T., Hohlfeld, K., Huq, M. S., Kanai, T., Laitano, F., Smyth, V.G. and Vynckier, S., Absorbed dose determination in external beam radiotherapy, International Atomic Energy Agency, Vienna, IAEA Technical Report Series No. 398, 2000.

[6] Evaluation of measurement data —Guide to the expression of uncertainty in measurement (GUM 1995 with minor corrections) JCGM 100: 2008.

[7] Burns, D. T. and Allisy-Roberts, P. J., The evaluation of degree of equivalence in regional dosimetry comparisons, 2007, CCRI(I)/07-04.

[8] Burns, D. T. and Butler, D., Updated report on the evaluation of degrees of equivalence in regional dosimetry comparisons, 2017, CCRI(I)/17-09.

Table 1. Participating laboratories and their contact persons for the APMP.RI(I)-K8 comparison

Participating Laboratory	Acronym or Abbreviation, Economy	Contact Person
International Atomic Energy Agency	IAEA, International organization	Ms Paula Toroi
Institute of Nuclear Energy Research	INER, Taiwan	Wei-Han Chu
Korea Research Institute of Standards and Science	KRISS, Korea	Chul-Young Yi
National Metrology Institute of Japan	NMIJ, Japan	Tadahiro Kurosawa
National Metrology Institute of South Africa	NMISA, South Africa	Sonwabile Arthur Ngcezu
National Research Council of Canada	NRC, Canada	Ernesto Mainegra-Hing
Malaysian Nuclear Agency	Nuclear Malaysia, Malaysia	Mohd Taufik Dolah
Pusat Teknologi Keselamatan dan Metrologi Radiasi - Badan Tenaga Nuklir Nasional	PTKMR-BATAN, Indonesia	C. Tuti Budiantari

Table 2. Schedule of APMP.RI(I)-K8 comparison

Participant	Date of chambers arriving at participant	Measurement at laboratory	Date of chambers leaving for the next participant
NMIJ		September 27, 2016	October 15, 2016
NRC	October 25, 2016	November 9, 2016	November 10, 2016
NMIJ	November 20, 2016	(not measured)	May 15, 2017
PTKMR-BATAN	October 16, 2017	October 23 to 27, 2017	October 30, 3017
NMISA	February 12, 2018	February 12 to 14, 2018	February 26, 2018
Nuclear Malaysia	March 9, 2018	April 9 to 13, 2018	April 16, 2018
INER	April 27, 2018	April 30 to May 4, 2018	May 7, 2018
NRC	May 18, 2018	May 21 to 25, 2018	June 6, 2018
IAEA	June 15, 2018	June 25, 2018	July 13, 2018
NMIJ	July 26, 2018	August 28 to 29, 2018	-*
KRISS	-*	September 18 to 21, 2018	

*KRISS performed measurements with their primary standard in Japan.

Table 3. Characteristics of the Standard Imaging well-chamber HDR 1000 Plus, ref. 90008

Characteristics	Nominal Value
Height of the chamber	15.6 cm
Diameter of the chamber	10.2 cm
Insert height	12.1 cm
Insert diameter	3.5 cm
Active volume	245 cm^3
Potential of HV electrode with respect to collecting electrode	-300 V

Table 4. Main characteristics of the HDR ^{192}Ir brachytherapy sources

Participant	After-loader unit	Manufacturer of source	Source type	Apparent activity of source	Capsule dimensions	capsule material	Source pellet dimensions
IAEA	Eckert & Ziegler BEBIG, SagiNova	Mallinckrodt Medical B.V.*3 , Eckert & Ziegler BEBIG GmbH	BEBIG HDR Ir-192	405.23 GBq (2017 Sep. 15)	0.9 mm diameter 4.52 mm length	Stainless steel AISI 316L	0.6 mm diameter 3.50 mm length
INER	Nucletron, microSelectron HDR-V2	Mallinckrodt Medical B.V., Elekta	microSelectron-HDR v2	525.4 GBq (2017 May 31)	0.9 mm diameter 4.5 mm length	Stainless steel AISI 316L	0.6 mm diameter 3.5 mm length
KRISS	Nucletron, microSelectron HDR-V2	Mallinckrodt Medical B.V., Elekta	microSelectron-HDR v2	152 GBq (2018 Aug. 29)	0.9 mm diameter 4.5 mm length	Stainless steel AISI 316L	0.6 mm diameter 3.5 mm length
NMIJ	Nucletron, microSelectron HDR-V2*1	Mallinckrodt Medical B.V., Elekta	microSelectron-HDR v2	158 GBq (2016 Sep. 27)	0.9 mm diameter 4.5 mm length	Stainless steel AISI 316L	0.6 mm diameter 3.5 mm length
NMIJ	Varian Medical Systems Inc. USA, Varisource*2	Varian Medical Systems Inc. USA	New VariSource HDR	126 GBq (2016 Sep. 27)	0.59 mm diameter 7.05 mm length	Nickel-Titanium alloy	0.34 mm diameter 5.0 mm length
NMISA	Eckert & Ziegler BEBIG, MultiSource	Mallinckrodt Medical B.V., Eckert & Ziegler BEBIG GmbH	BEBIG HDR Ir-192	423.50 GBq (2017 May 3)	0.9 mm diameter 4.52 mm length	Stainless steel AISI 316L	0.6 mm diameter 3.5 mm length
NRC	Nucletron, microSelectron HDR-V2	Mallinckrodt Medical B.V., Elekta	microSelectron-HDR v2	434.08 GBq (2017 Nov. 6)	0.9 mm diameter 4.5 mm length	Stainless steel AISI 316L	0.6 mm diameter 3.5 mm length
Nuclear Malaysia	Nucletron, microSelectron HDR-V3	Mallinckrodt Medical B.V., Elekta	microSelectron-HDR v2	503.0 GBq (2018 Mar. 13)	0.9 mm diameter 4.5 mm length	Stainless steel AISI 316L	0.6 mm diameter 3.5 mm length
PTKMR-BATAN	Nucletron, microSelectron HDR-V2	Mallinckrodt Medical B.V., Elekta	microSelectron-HDR v2	511.6 GBq (2017 Aug. 2)	0.9 mm diameter 4.5 mm length	Stainless steel AISI 316L	0.6 mm diameter 3.5 mm length

*1 NMIJ measured the calibration coefficients two times for the microSelectron mHDR-V2 source. The second measurement was performed using the same model but a different source from the first measurement.

*2 The Varisource was used for checking the well-chamber response to different source types. The calibration coefficients of NMIJ were derived only from the measurements using the microSelection mHDR-V2 source.

*3 New name since 2020: Curium Netherlands B.V.

Table 5. Standard traceability and method to determine the reference air kerma rate. Where non-primary methods were used, the calibration source type at the calibration provider is stated.

Participant	Standard traceability (source type)	Method of RAKR determination
IAEA	PTB (microSelectron-HDR v2)	Secondary standard well-type chamber calibrated for ^{192}Ir
INER	INER	Primary standard cavity chamber
KRISS	KRISS	Primary standard cavity chamber
NMIJ	NMIJ	Primary standard cavity chamber
NMISA	PTB (microSelectron-HDR v2)	Secondary standard well-type chamber calibrated for ^{192}Ir
NRC	NRC	Primary standard cavity chamber (S_K, multiple-distance method)
Nuclear Malaysia	University of Wisconsin-Madison (BEBIG HDR Ir2.A85-2)	Secondary standard well-type chamber calibrated for ^{192}Ir
PTKMR-BATAN	University of Wisconsin-Madison (BEBIG HDR Ir2.A85-2)	Secondary standard well-type chamber calibrated for ^{192}Ir

Table 6. Key comparison ratios NMI/BIPM of reference air-kerma for HDR ^{192}Ir brachytherapy for NMIJ and NRC [1]

Laboratory	$R_{\mathrm{LINK,BIPM}}$	Combined standard uncertainty u_c
BIPM	-	0.0026
NMIJ	1.0036	0.0054
NRC	0.9966	0.0050

Table 7. The calibration coefficients ($N_{K,\mathrm{NMI}}$) of the transfer chambers for the APMP.RI(I)-K8 key comparison

Participant	$N_{K,\mathrm{NMI}}$ (10^5 Gy m^2 h^{-1} A^{-1})		Relative expanded uncertainty (%, k = 2)
	A153466	A983216	
IAEA	4.68	4.66	2.8
INER	4.68	4.66	1.5
KRISS	4.65	4.64	1.1
NMIJ	4.67	4.66	1.1
NMISA	4.67	4.65	2.8
NRC	4.60	4.58	1.4
Nuclear Malaysia	4.61	4.59	2.9
PTKMR-BATAN	4.86	4.77	3.1

Table 8. Comparison ratios between participants and the BIPM using the value of the linking laboratory NMIJ

Participant	$R_{NMI,LINK}$			$(R_{NMI,BIPM})_i$
	A153466	A983216	Mean	
IAEA	1.0014	1.0008	1.0011	1.0047
INER	1.0020	1.0016	1.0018	1.0054
KRISS	0.9959	0.9961	0.9960	0.9996
NMISA	0.9990	0.9991	0.9991	1.0027
Nuclear Malaysia	0.9858	0.9851	0.9855	0.9890
PTKMR-BATAN	1.0400	1.0245	1.0323	1.0360

Table 9. Comparison ratios between participants and the BIPM using the value of the linking laboratory NRC

Participant	$R_{NMI,LINK}$			$(R_{NMI,BIPM})_i$
	A153466	A983216	Mean	
IAEA	1.0174	1.0176	1.0175	1.0141
INER	1.0181	1.0184	1.0183	1.0148
KRISS	1.0119	1.0129	1.0124	1.0089
NMISA	1.0151	1.0159	1.0155	1.0120
Nuclear Malaysia	1.0016	1.0017	1.0017	0.9983
PTKMR-BATAN	1.0567	1.0418	1.0493	1.0457

Table 10. Combined comparison ratios $\overline{R_{NMI,BIPM}}$ between participants and the BIPM using the unweighted mean for the two linking laboratories from Tables 7 and 8.

Participant	$\overline{R_{NMI,BIPM}}$	$u_{R,NMI}$
IAEA	1.0094	0.0152
INER	1.0101	0.0098
KRISS	1.0042	0.0082
NMISA	1.0073	0.0152
Nuclear Malaysia	0.9936	0.0154
PTKMR-BATAN	1.0408	0.0172

Table 11. Degree of equivalence of the participating NMIs with respect to the BIPM reference value

Participant	D_i /(mGy/Gy)	U_i
IAEA	9.4	30.5
INER	10.1	19.6

KRISS	4.2	16.4
NMIJ*	3.6	10.8
NMISA	7.3	30.5
NRC*	-3.4	10.0
Nuclear Malaysia	-6.4	30.8
PTKMR-BATAN	40.8	34.3

*Determined in BIPM.RI(I)-K8 comparisons

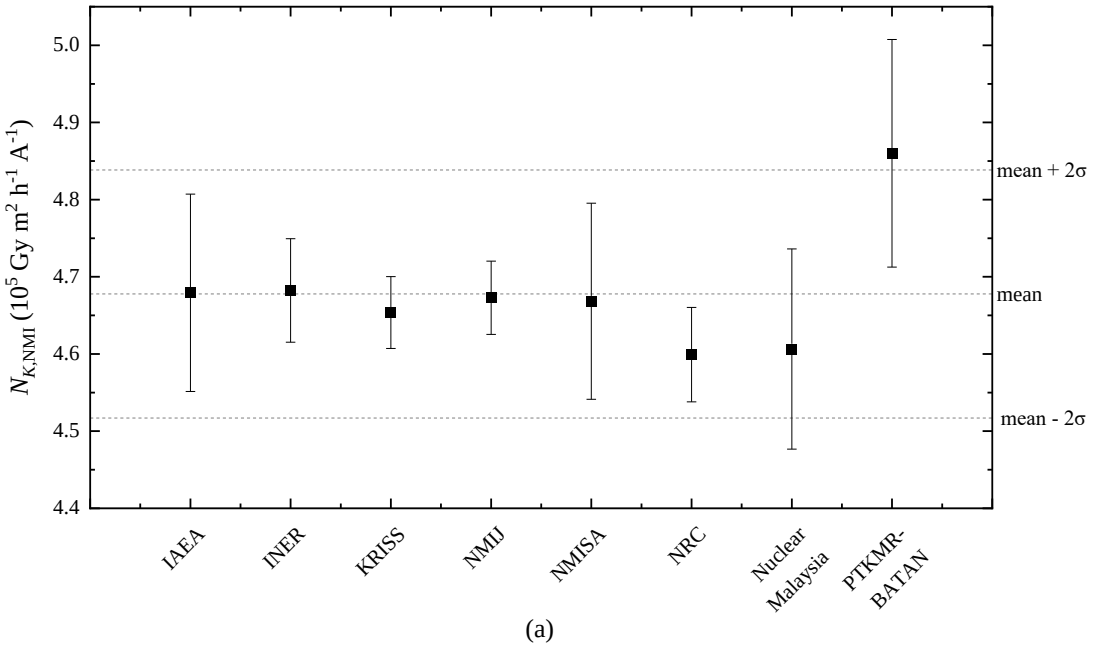

(a)

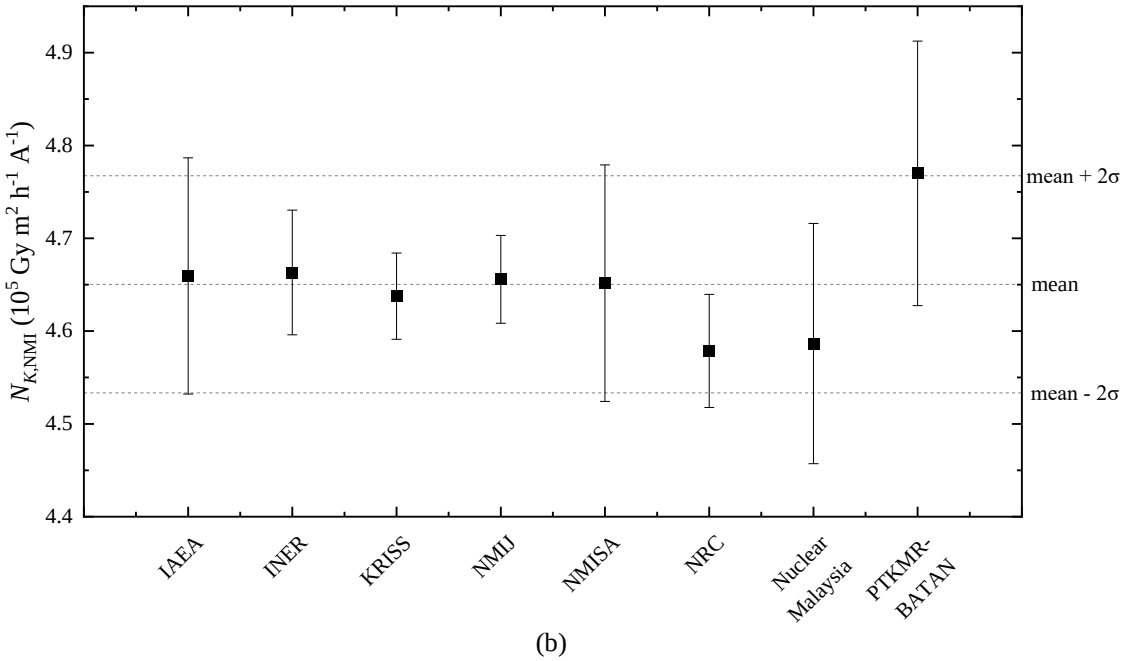

(b)

Figure 1. The distribution of the transfer chamber calibration coefficients ($N_{K,NMI}$) with two standard deviations of the distribution indicated. The error bars represent the expanded uncertainty (k = 2). (a) A153466 (b) A983216

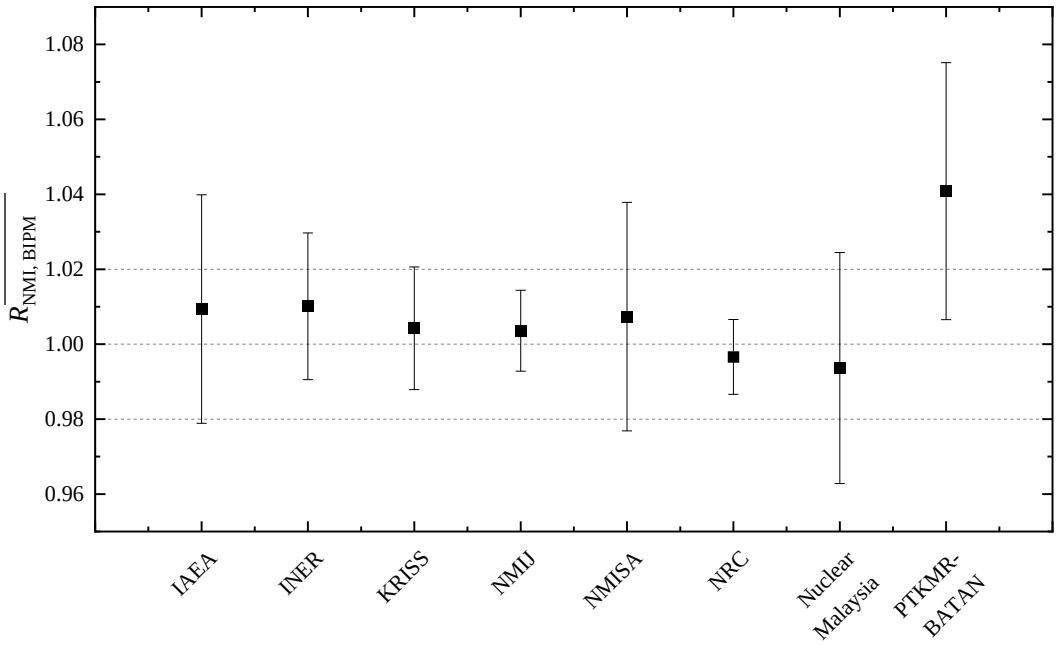

Figure 2. Final results $\overline{R_{\mathrm{NMI,BIPM}}}$ for each participating laboratory for the APMP.RI(I)-K8 comparison. The error bars represent the expanded uncertainty (k = 2). NMIJ and NRC values are from the respective BIPM.RI(I)-K8 comparisons.

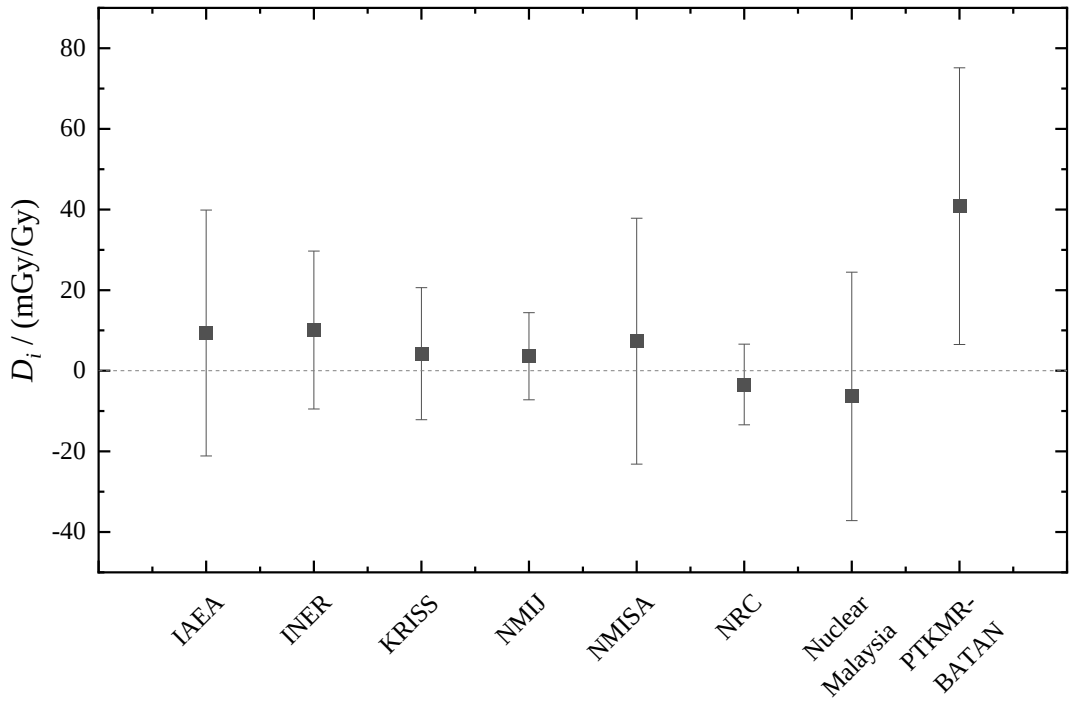

Figure 3. Degree of equivalence D_i and U_i for the participating laboratories with respect to the BIPM reference value. The error bars represent the expanded uncertainty (k = 2).

Appendix I

IAEA Uncertainty budget

Uncertainties associated with the RAKR determination of ^{192}Ir source

Component	Relative standard uncertainty (%)	
	Type A	Type B
calibration coefficient		1.25
long term stability Ref. Std.		0.1
recombination losses		0.04
pressure		0.1
temperature		0.2
radioactive decay of the source		0.2
source position		0.01
ionization current	0.01	0.1
metal needle (LLA210-S)		0.30
Quadratic sum	0.01	1.33
Combined standard uncertainty	1.33	

Uncertainty associated with the calibration of the transfer chambers

Component	Relative standard uncertainty (%)	
	Type A	Type B
determination of RAKR	0.01	1.33
ionization current	0.01	0.1
pressure		0.1
temperature		0.2
recombination losses		0.04
radioactive decay of the source		0.2
source position		0.01
Quadratic sum	0.01	1.37
Combined standard uncertainty	1.37	

INER Uncertainty budget

Uncertainties associated with the RAKR determination of ^{192}Ir source

Component	Relative standard uncertainty (%)	
	Type A	Type B
Physical Constants		
dry air density		0.01
ratio of mass energy-absorption coefficients		0.11
ratio of mass stopping powers mean energy per charge		0.13
fraction of energy lost by bremsstrahlung		0.02
Correction factors		
humidity		0.05
pressure		0.05
temperature		0.024
recombination losses		0.015
wall attenuation and scattering		0.15
stem scattering	0.17	
air attenuation		0.01
axial non-uniformity		0.11
radial non-uniformity		0.02
barometer calibration		0.01
thermometer calibration		0.14
central electrode correction		0.06
polarity correction		0.18
scatter correction		0.27
radioactive decay of the source		0.02
positioning correction		0.06
Measurements		
chamber volume		0.023
ionization current	0.047	
measurement time		0.04
long-term stability	0.5	
Quadratic sum	0.53	0.45
Combined standard uncertainty	0.70	

Uncertainty associated with the calibration of the transfer chambers

Component	Relative standard uncertainty (%)	
	Type A	Type B
determination of RAKR	0.53	0.45
ionization current	0.092	
pressure		0.010
temperature		0.036
recombination correction		0.15
calibration coefficient of participant's electrometer		0.010
radioactive decay of the source		0.020
Quadratic sum	0.54	0.48
Combined standard uncertainty	0.72	

KRISS Uncertainty budget

Uncertainties associated with the RAKR determination of ^{192}Ir source

Component	Relative standard uncertainty (%)	
	Type A	Type B
Physical Constants		
dry air density		0.01
ratio of mass energy-absorption coefficients		0.06
ratio of mass stopping powers mean energy per charge		0.15
fraction of energy lost in radiative processes		0.02
Correction factors		
humidity		0.03
pressure		0.1
temperature		0.1
recombination losses	0.01	0.02
wall attenuation and scattering	0.05	0.15
stem scattering	0.06	0.1
air attenuation and scattering	0.1	0.3
axial and radial non-uniformity	0.01	0.1
Measurements		
chamber volume	0.02	0.09
ionization current	0.02	0.04
Quadratic sum	0.13	0.44
Combined standard uncertainty	0.46	

Uncertainty associated with the calibration of the transfer chambers

Component	Relative standard uncertainty (%)	
	Type A	Type B
determination of RAKR	0.13	0.44
ionization current	0.01	0.05
pressure		0.1
temperature		0.1
recombination correction	0.01	0.02
calibration coefficient of electrometer		0.12
radioactive decay of the source		0.05
Quadratic sum	0.13	0.48
Combined standard uncertainty	0.50	

NMIJ Uncertainty budget

Uncertainties associated with the RAKR determination of ^{192}Ir source

Component	Relative standard uncertainty (%)	
	Type A	Type B
Physical Constants		
dry air density		0.01
ratio of mass energy-absorption coefficients		0.12
ratio of mass stopping powers mean energy per charge		0.15
fraction of energy lost in radiative processes		0.02
Correction factors		
humidity		0.03
pressure		0.1
temperature		0.1
recombination losses		0.05
wall attenuation and scattering	0.1	0.14
stem scattering		0.15
air attenuation and scattering	0.1	0.14
axial and radial non-uniformity		0.1
Measurements		
chamber volume	0.01	0.03
ionization current	0.1	0.23
Quadratic sum	0.17	0.43
Combined standard uncertainty	0.47	

Uncertainty associated with the calibration of the transfer chambers

Component	Relative standard uncertainty (%)	
	Type A	Type B
determination of RAKR	0.17	0.43
ionization current	0.03	
pressure		0.2
temperature		
recombination correction	0.0008	
calibration coefficient of electrometer		0.025
radioactive decay of the source		0.04
Quadratic sum	0.18	0.48
Combined standard uncertainty	0.51	

NMISA Uncertainty budget

Uncertainties associated with the RAKR determination of ^{192}Ir source

Component	Relative standard uncertainty (%)	
	Type A	Type B
calibration coefficient		1.25
pressure		0.005
temperature		0.046
sweet spot determination		0.087
drift of standard	0.5	
Quadratic sum	0.50	1.25
Combined standard uncertainty	1.35	

Uncertainty associated with the calibration of the transfer chambers

Component	Relative standard uncertainty (%)	
	Type A	Type B
determination of RAKR	0.50	1.25
pressure		0.005
temperature		0.046
sweet spot determination		0.213
recombination factor		0.025
stability of charge measurements	0.076	
Quadratic sum	0.51	1.27
Combined standard uncertainty	1.37	

NRC Uncertainty budget

Uncertainties associated with the RAKR determination of ^{192}Ir source

Component	Relative standard uncertainty (%)	
	Type A	Type B
2S ^{192}Ir calibration factor		0.39
S_K/N_K NLLS fit std		0.32
ionization current	0.01	
pressure and temperature correction	0.01	0.07
multiple source-detector distances	0.40	
Seed exp. positioning repeatability	0.10	
Repeatability		0.07
Quadratic sum	0.41	0.51
Combined standard uncertainty	0.66	

Uncertainty associated with the calibration of the transfer chambers

Component	Relative standard uncertainty (%)	
	Type A	Type B
Determination of RAKR	0.41	0.51
Ionization current	0.03	0.03
Pressure and temperature correction	0.05	0.10
Distance	0.02	0.02
Quadratic sum	0.42	0.52
Combined standard uncertainty	0.67	

Nuclear Malaysia Uncertainty budget

Uncertainties associated with the RAKR determination of ^{192}Ir source

Component	Relative standard uncertainty (%)	
	Type A	Type B
calibration coefficient		1.3
pressure		0.003
temperature		0.14
recombination losses		0.22
radioactive decay of the source		0.09
ionization current	0.02	
Quadratic sum	0.02	1.33
Combined standard uncertainty	1.33	

Uncertainty associated with the calibration of the transfer chambers

Component	Relative standard uncertainty (%)	
	Type A	Type B
determination of RAKR		1.33
ionization current	0.003	
pressure		0.003
temperature		0.14
recombination correction		0.43
radioactive decay of the source		0.09
Quadratic sum	0.003	1.41
Combined standard uncertainty	1.41	

PTKMR-BATAN Uncertainty budget

Uncertainties associated with the RAKR determination of ^{192}Ir source

Component	Relative standard uncertainty (%)	
	Type A	Type B
calibration coefficient		1.4
ionization current	0.1	0.02
pressure temperature		0.04
recombination losses		0.03
radioactive decay of the source		0.01
long-term stability of the secondary standard		0.15
setup and source positioning		0.2
Quadratic sum	0.10	1.42
Combined standard uncertainty	1.43	

Uncertainty associated with the calibration of the transfer chambers

Component	Relative standard uncertainty (%)	
	Type A	Type B
determination of RAKR	0.1	1.42
ionization current	0.1	0.01
pressure temperature		0.037
recombination correction		0.04
radioactive decay of the source		0.4
calibration coefficient of electrometer		0.25
setup and source positioning		0.2
Quadratic sum	0.1	1.51
Combined standard uncertainty	1.52	